A La_2NiO_4-zeolite membrane reactor for the CO_2 reforming of methane to syngas

B.S. Liu and C.T. Au *

Department of Chemistry and Centre for Surface Analysis and Research, Hong Kong Baptist University, Kowloon Tong, Hong Kong, China
E-mail: pctau@hkbu.edu.hk

Received 24 April 2001; accepted 7 August 2001

The La_2NiO_4-zeolite membrane was prepared by means of *in situ* hydrothermal synthesis. Techniques such as XRD, SEM-EDX, and BET were used to acquire information as related to the structure, morphology and the pore size distribution of the membrane. At room temperature, we observed a H_2/CH_4 separation factor of 9.2, considerably higher than the Knudsen diffusion value. With the simultaneous separation of CO and H_2 in the membrane reactor, both CO_2 and CH_4 conversions were enhanced in the CH_4/CO_2 reforming reaction.

KEY WORDS: CO_2/CH_4 reforming; La_2NiO_4-zeolite membrane; membrane reactor; hydrothermal synthesis

1. Introduction

During the past two decades, the CO_2 reforming of methane has attracted much attention from both industrial and environmental sectors. In the environmental aspect, both CO_2 and methane are undesirable greenhouse gases, and the reforming reaction provides a way for CO_2 utilization. From the industrial viewpoint, the conversion of methane and CO_2 into value-added products is desirable since the two gases are cheap and abundant. Synthesis gas (*i.e.*, $CO + H_2$) can be used in chemical energy transmission systems [1,2] or utilized in the Fischer–Tropsch reaction [3,4].

In recent years, a variety of catalysts have been developed for CH_4/CO_2 reforming. Although catalysts of supported noble metals (such as Rh [5,6], Ru [7,8], Pd [9]) are promising, the high costs of the precious metals limit their application. From the commercial standpoint, it is more profitable to develop the nickel-based catalysts. The problem with the supported nickel catalysts is easy deactivation due to coking, a consequence of nickel sintering and carbon deposition. Lately, Choudhary *et al.* reported that complex oxides, such as $LaNiO_3$, $La_{0.8}Ca(\text{or Sr})_{0.2}NiO_3$, $LaNi_{1-x}Co_xO_3$ (where $x = 0.2$–1) [10] with perovskite structure were resistant to coking. In addition, Bolt *et al.* [11] observed that the extent of nickel sintering was reduced over the $NiAl_2O_4$ catalyst with discontinuous interfacial layers.

In recent years, the coupling of catalytic action with membrane separation is becoming feasible for practical application. According to Le Chatelier–Braun's law, if a specified product was separated at equilibrium from a system, the chemical reaction moves towards the direction of production. It has been pointed out that in the steam reforming of methane, up to 100% CH_4 conversion can be accomplished in a palladium membrane reactor at 500 °C with no carbon deposition [12]. In the application of a dense palladium membrane reactor for the generation of syngas from methane, Galuszka *et al.* [13] observed the swelling and consequently the destruction of the membrane due to the generation of filamentous carbon. It seems that a palladium membrane is not suitable in CH_4/CO_2 reforming. Currently, composite membranes, consisting of thin layers of zeolite films on a porous supporting structure, are being developed as an alternative. Molecules are separated on the basis of molecular size through these porous membranes. Yan *et al*. [14] have prepared a ZSM-5 membrane on porous alumina with good permeaselectivity (permeance at 185 °C, 10.1×10^{-8}, 5.9×10^{-8} and 0.19×10^{-8} mol m^{-2} s^{-1} Pa^{-1}, for hydrogen, *n*-butane and isobutane, respectively) by *in situ* hydrothermal synthesis. Matsukata *et al*. [15] have prepared a crackless zeolite membrane on porous alumina, with the thickness of the zeolite membranes being in the range of 40–500 μm. Further study of the mechanism of thin layer formation is likely to lead to thinner and better permeable membranes of this kind. In the literature, reports on the preparation and performance of zeolite membranes are mainly related to the perevaporation of ethanol and water [16].

The use of membrane as an intrinsically active catalyst or as a catalyst support has not been very successful. To our knowledge, the study on CO_2 reforming of methane over a catalytic membrane reactor has not been reported before. In this paper, the defect-free zeolite membranes were prepared by means of *in situ* hydrothermal synthesis and applied in CO_2 reforming of methane; we observed that CH_4 and CO_2 conversions were significantly higher than those recorded over a common fixed-bed reactor.

* To whom correspondence should be addressed.

1011-372X/01/1100-0067$19.50/0

2. Experimental

2.1. Preparation of zeolite membranes

The mixture for synthesis was prepared by the addition of an aluminum sol generated from aluminum hydroxide to a solution of sodium meta-silicate; the mixture was then stirred for 30 min before use (molar ratios $SiO_2/Al_2O_3 = 5$, $Na_2O/SiO_2 = 1.0$ and $H_2O/Na_2O = 120$).

Zeolite membranes were prepared on two types of α-Al_2O_3 ceramic tubes according to the *in situ* crystallization procedure. The first was a porous α-Al_2O_3 tube (ID 8 mm, OD 12 mm and length 100 mm), and the average pore diameter and porosity of the alumina support were about 0.2 μm and 40%, respectively. The second was an α-Al_2O_3 tube coated with a layer of γ-Al_2O_3 by means of the sol–gel method previously reported [17]. The average pore size and porosity of this support tube were about 3–5 nm and 35%. The thickness of the γ-Al_2O_3 layer was about 10 μm.

For the coating of the membrane, the outer wall of a dried ceramic tube with both ends open was wrapped with two layers of commercial Teflon tape, and was placed vertically in an autoclave. The synthesis mixtures were poured into the autoclave so that the upper opening of the tube was approximately 2–3 mm beneath the mixture level. Subsequently, the autoclave was closed and placed in an oven, which had been pre-heated to the required synthesis temperature. The zeolite membrane was synthesized *in situ* under autogenous pressure. At the end of a chosen synthesis time, the autoclave was quenched in cool water and the tube deposited with zeolite membrane was removed from the autoclave. Both the membrane tube and loose zeolite crystalline deposited on the bottom of the autoclave were rinsed with deionized water until the pH of the rinse water reached a value lower than 8. Subsequently, they were dried overnight in air at 60 or 100 °C. The synthesis procedure could be repeated three or four times on a membrane tube to generate sequential layers of coating and to fill up cracks that might be formed during drying. The procedure is referred to as repeated synthesis.

2.2. Preparation of La_2NiO_4 catalytic membrane

The gel of $La(NO_3)_3 + Ni(NO_3)_2{\cdot}6H_2O$ was prepared by the citrate method. In this method, stoichiometric metal nitrates, like $Ni(NO_3)_2{\cdot}6H_2O$, $La(NO_3)_3$ (molar ratio of Ni and La is 1 : 2) were fully dissolved in diluted nitric acid, followed by the addition of citric acid and ethylene glycol. The molar amounts of citric acid and ethylene glycol were 1.5 times that of the total metal ions. Then the obtained solution was heated with stirring to 90 °C. After the solution was isothermally stirred and refluxed for 3 h, with the removal of water through evaporation, a sticky gel was formed.

The La_2NiO_4/zeolite composite membrane was prepared on an alumina tube that was covered with zeolite membrane by the impregnation of the aforementioned gel. The catalytic membrane precursor was dried at 110 °C overnight, and then placed in a furnace with temperature increased to 800 °C at a rate of 100 °C h^{-1} and kept at this temperature for 2 h.

2.3. Preparation of 9% NiO–La_2O_3/γ-Al_2O_3 catalysts

The 9% NiO–La_2O_3/γ-Al_2O_3 catalyst was prepared by means of sol–gel processing of organometallic precursors according to the following procedure. 20 g aluminum isopropoxide was hydrolyzed with 150 ml of deionized water at 80 °C in a flask, and the mixture was kept at 80 °C for 1.5 h with vigorous stirring. Then, 0.01 mol of nitric acid was added for peptization and the sol was refluxed at 95 °C for 1 h with stirring to obtain a clear sol. Then 6.49 and 5.8 g of $Ni(NO_3)_2{\cdot}6H_2O$ and La_2O_3 were dissolved, respectively, in 15 ml of 20% HNO_3. This solution was then added to the clear boehmite sol and the mixture was refluxed at 95 °C for 16 h with vigorous stirring. The obtained cogel was put in a beaker for solvent evaporation at room temperature (RT). Finally, the dry cogel was calcined at 500 °C for 6 h.

2.4. Characterization of zeolite membrane

The zeolite membrane and powder generated during the synthesis of the membrane, as well as the catalysts were characterized by X-ray diffraction (XRD, Rigaku D-max) technique with Cu Kα radiation.

The surface and cross-section morphology of the membrane was examined by means of scanning electron microscopy (SEM, Jeol JSM-T330A) operating at 20 kV. The Si, Al and Na concentrations on the surface of the membrane were measured by means of energy dispersive X-ray analysis (EDX). The adsorption–desorption isotherm of N_2 and pore size distribution for the zeolite membranes were measured using N_2 as the adsorbate on a NOVA-1200 instrument at 77 K.

2.5. Permeation measurements

Single-gas permeation of H_2, CH_4, CO_2 and CO was measured over a temperature range of RT $\approx$ 700 °C. The membrane was sealed in a stainless-steel module by silicone O-rings, then the pure gas was introduced into the inner tube and permeated through the membrane into the outer tube; the pressure drop from feed to permeation side was 17.24 kPa. The permeance of H_2, CO, CH_4 and CO_2 through the zeolite membrane was separately determined by means of a soap-bubble flowmeter. The ratio of the permeances of two single gases is defined as the ideal separation factor.

A similar module was used for the separation of the binary gas mixture. In order to simulate gas resistance in a catalytic reaction, the downstream outlet of the feed side was blocked with quartz wool. The total feed rate for binary gas mixture (1 : 1) was 50 ml min^{-1}, and nitrogen was used as the sweeping gas. The gas mixtures in permeation and feeding sides were analyzed, respectively, by gas chromatography (Shimadzu 8A, TCD, Porapak Q packed column). The

separation factor for two mixture gases was calculated according to the following equation:

$$\text{separation factor} = \frac{(X_i/X_j)_{\text{permeate}}}{(X_i/X_j)_{\text{feed}}},$$

where X_i and X_j represent mole fraction of i and j species, respectively.

2.6. Evaluation of catalytic activity and coke deposition

For comparison, we first conducted an initial study on the performance of the 9% NiO–La_2O_3/γ-Al_2O_3 catalyst over a fixed-bed reactor under the condition of gas hour space velocity (GHSV) equaled 4.8×10^4 ml g^{-1} h^{-1}.

The membrane reactor was installed with a porous permeable La_2NiO_4 zeolite membrane tube capable of withstanding high temperature (figure 1). The 9% NiO–La_2O_3/γ-Al_2O_3 catalyst (0.2 g) was packed in the inner part of the La_2NiO_4–zeolite membrane tube. The gas mixture of methane and CO_2 (1 : 1) was fed to the membrane reactor from the inlet (inner path) at a GHSV of 4.8×10^4 ml g^{-1} h^{-1}. Part of the hydrogen and carbon monoxide produced permeated through the zeolite membrane into the outer tube, where they were carried away by sweeping nitrogen.

The reactants and products were analyzed by means of on-line gas chromatography (Shimadzu 8A, TCD). A Porapak Q and a 5 A sieve column were used for gas separation. Since H_2, CO, N_2, CH_4 and CO_2 permeate through the membrane in different permeability, the effluents from the inner and outer path were analyzed, respectively.

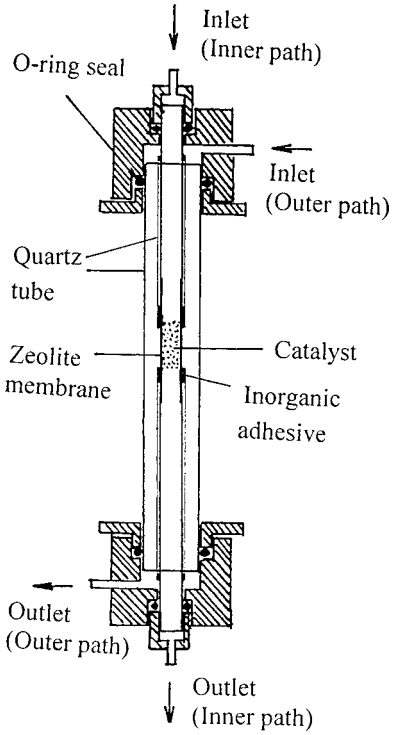

Figure 1. Schematic diagram of membrane reactor for CH_4/CO_2 reforming.

3. Results and discussion

3.1. Structure and morphology of zeolite membrane

The XRD patterns of the α-Al_2O_3 support, the as-synthesized zeolite membrane, and zeolite powder are shown in figure 2. The XRD pattern of the α-Al_2O_3 support was identical with that described by Thompson *et al.* [18]. As expected, randomly oriented zeolite membranes were formed on the α-Al_2O_3 support (figure 2(b)) and the XRD lines of the support were rather strong, indicating that the zeolite layers were rather thin. The diffraction peaks of zeolite powder appeared (figure 2(c)) at the angle of $2\theta = 10.0°$, 11.7°, 15.4°, 20.3°, 23.4°, 26.7° and 31.0°, confirming that the zeolite NaY membrane was mainly originated from silica-aluminate sol, in agreement with the results of Armstrong *et al.* [19]. The results of EDX analysis indicated that the SiO_2/Al_2O_3 ratio on the surface of the zeolite membrane was 3.4. However, without proper aging, the SiO_2/Al_2O_3 ratio was 1.7 accompanied with the presence of zeolite P particles as a contaminant. As pointed out later, the SEM results revealed that there were zeolite P particles (marked by an arrow in figure 3(d)) at different positions of the zeolite membrane.

We investigated the shape and the size distribution of the crystallites of the samples by means of scanning electron microscopy (SEM-EDX). The photograph of the porous support, the surface and cross-section of the zeolite membrane

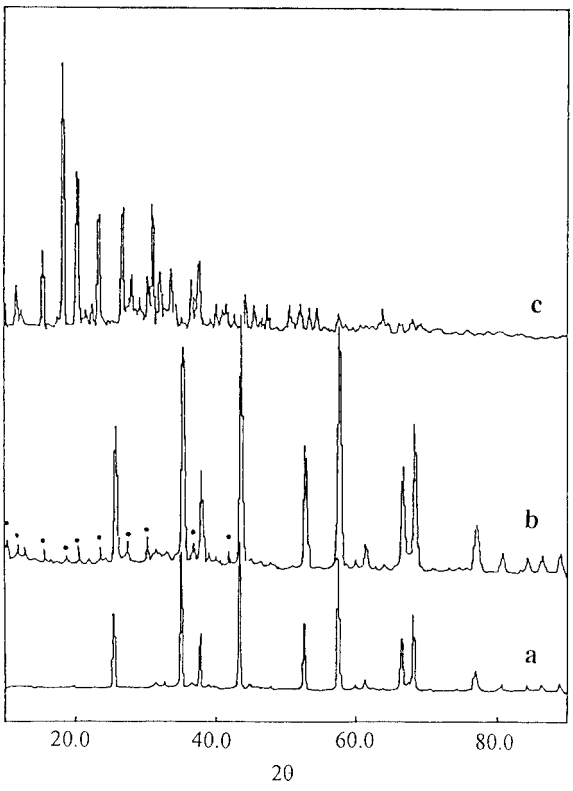

Figure 2. XRD patterns of (a) α-Al_2O_3 support, (b) zeolite membrane on α-Al_2O_3 support and (c) zeolite powder obtained from the parent solution of synthesized zeolite membrane.

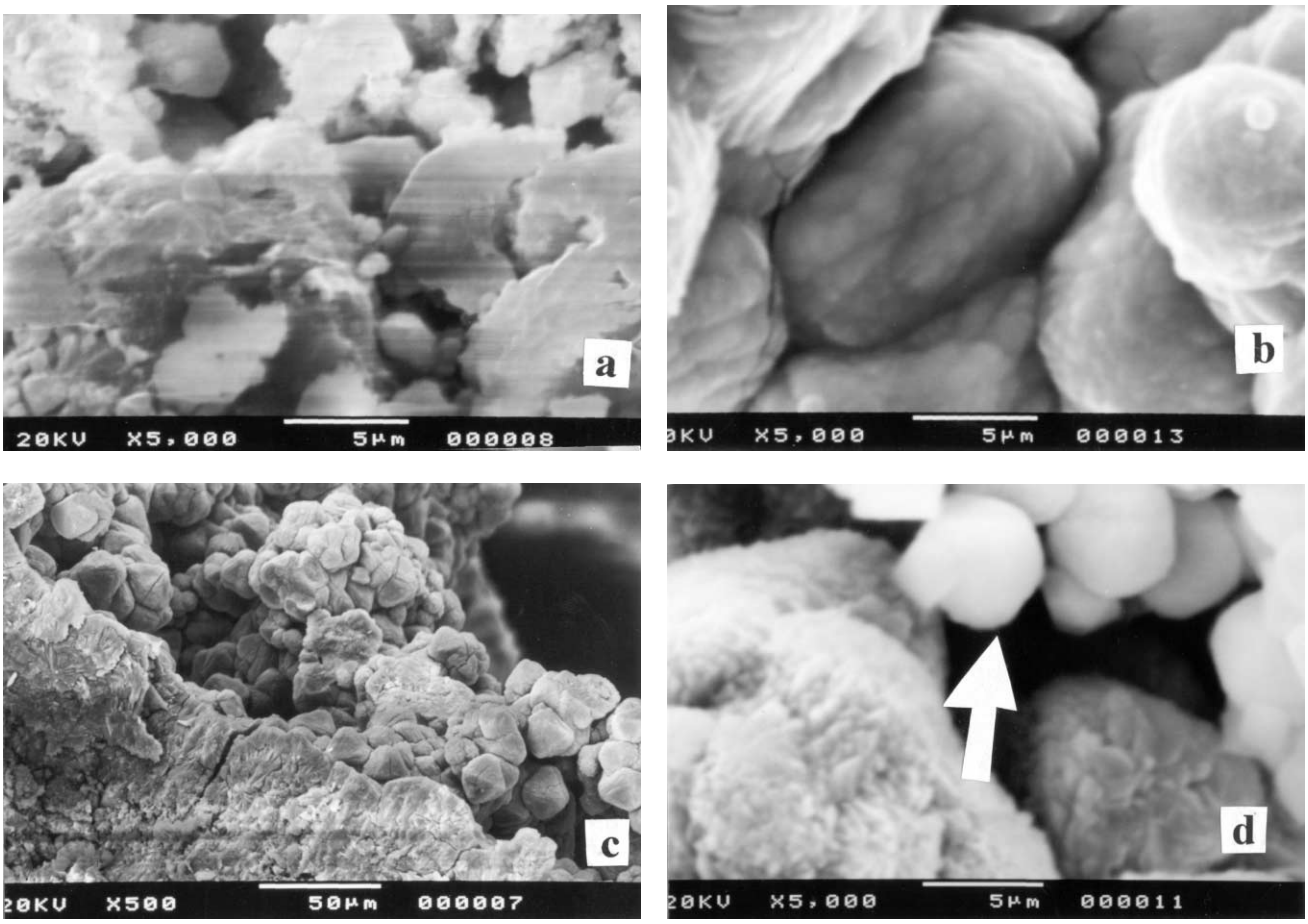

Figure 3. SEM photographs of (a) α-Al_2O_3 support, (b) cross-section of zeolite membrane, (c) top surface of the membrane obtained by means of repeated synthesis (three times) and (d) zeolite P particles appeared as a contaminant during hydrothermal synthesis.

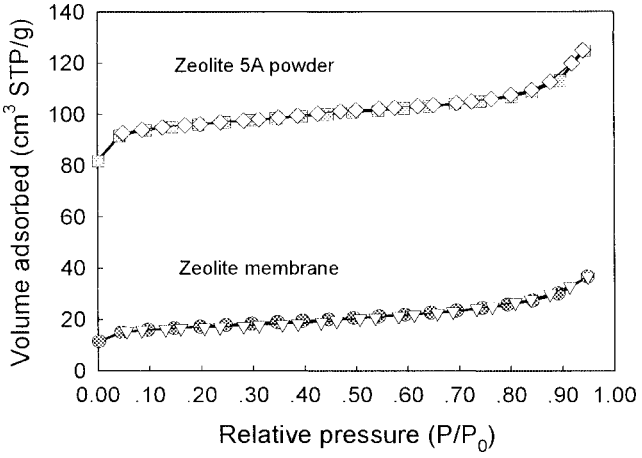

Figure 4. Nitrogen adsorption–desorption isotherm at 77 K.

after crystallization for 34 h are shown in figure 3. We observed the zeolite NaY crystallites in well-defined octahedral planes (figure 3(c)). The average size of the particles was within the 5–10 μm range, larger than the values previously reported by Interrante *et al.* [20]. It is known that the shape and the particle size of the zeolite are dependent on the growth condition as well as the amount of water in the silica-aluminate sol. The thickness of the zeolite membrane after two times of crystallization was about 60 μm. After 34 h of membrane synthesis, the inner surface of the porous support was completely covered with randomly oriented zeolite and a prolonged crystallization time would result in the growth of P-type zeolite as mentioned before (figure 3(d)).

In order to elucidate the pore structure of the zeolite membrane, the adsorption–desorption isotherm of N_2 was investigated and the results are depicted in figure 4. It can be seen that similar to the results of zeolite 5A powder, the isotherm of the zeolite membrane remained nearly horizontal over a large P/P_0 range, indicating that most of the adsorption took place at the low pressure region and the pore volume was well defined. The results implied a type I physisorption isotherm of microporous solid with relatively small external surface (according to the IUPAC classification [21]), and the sample consisted of micropores with pore diameter of less than 2 nm [22]. However, one can learn from the pore size distribution curves (figure 5) of the zeolite membrane that besides the micropores, there were some mesopores of around 3.5 nm, possibly related to cracking created during drying. In addition, although the pore size of micropore zeolite cannot be determined by means of N_2 adsorption, the micropore volume of a zeolite membrane can be estimated by the t-method of Halsey [23].

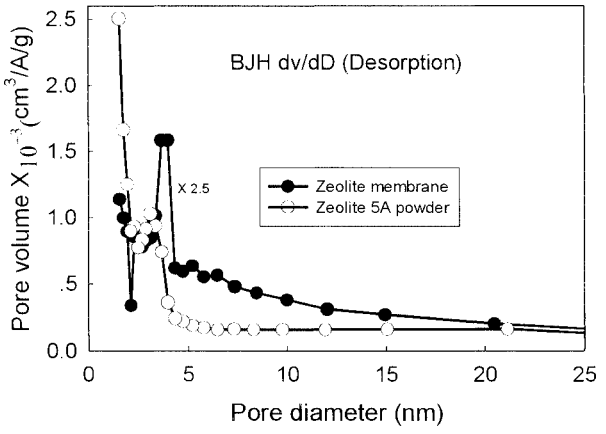

Figure 5. Pore size distribution curves for zeolite membrane (•) and zeolite 5A powder (○).

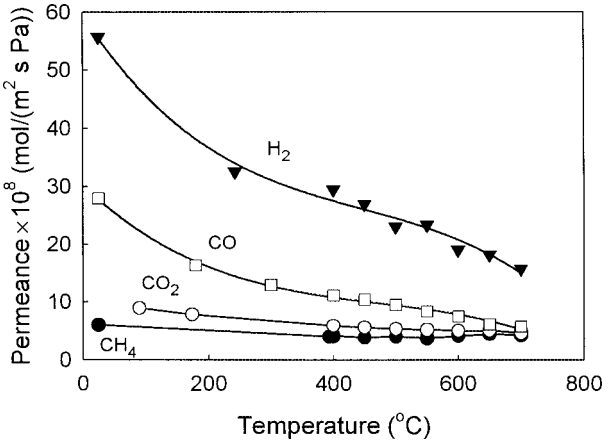

Figure 6. Permeance of single gas through the zeolite membrane as a function of temperature.

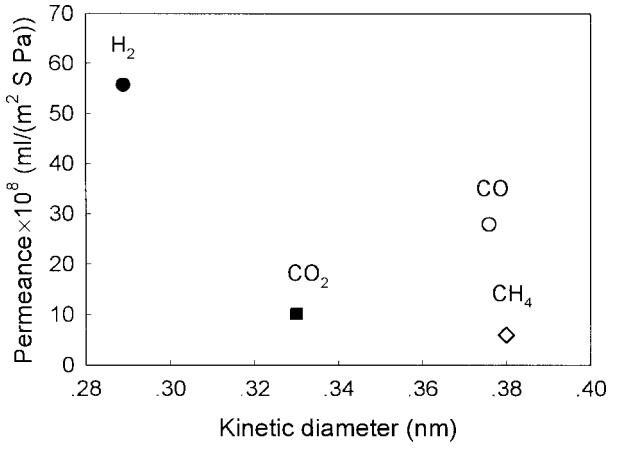

Figure 7. Relationship of the permeance of single gas with the kinetic diameter of the molecule.

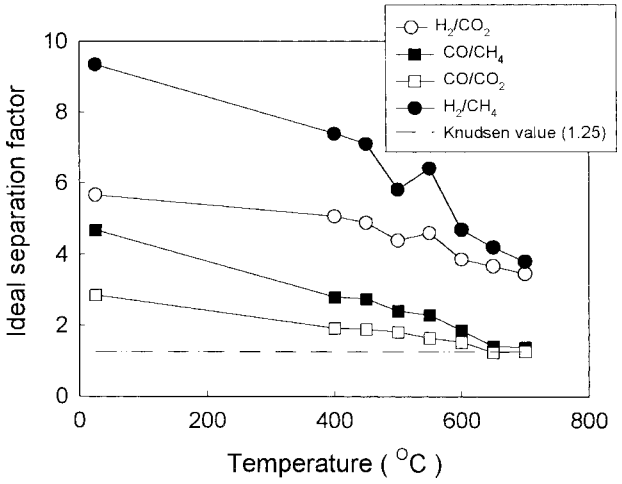

Figure 8. Ideal separation factor as a function of temperature.

3.2. Permeation of single gases

The gas permeation test was performed on the zeolite membrane reactor with no catalyst at different temperatures. Figure 6 indicated that the permeance of H_2 through the single-coated zeolite membrane was 5.5×10^{-7} mol m^{-2} s^{-2} Pa^{-1}, which was significantly lower than that through the support ($\sim 5 \times 10^{-6}$ mol m^{-2} s^{-2} Pa^{-1}). Meanwhile, for CH_4 and CO_2, the permeances at RT were 6×10^{-8} and 9×10^{-8} mol m^{-2} s^{-2} Pa^{-1}, respectively; the corresponding permeaselectivity of H_2/CH_4 was up to 9.2, much higher than the value (2.8) governed by the mechanism of Knudsen diffusion. The results suggested that the zeolite membrane that had been synthesized repeatedly for three times was defect-free, as confirmed by SEM. However, with increasing temperature, the permeances of H_2 and CO through the zeolite membrane decreased whereas those of CO_2 and CH_4 remained roughly constant. According to the diffusion theory of gas, the gas permeances of Knudsen flow in mesopores (pore size 2–20 nm) should decrease gradually with temperature rise (permeances proportional to $T^{-1/2}$ [24]). This indicated that the permeance of small molecules with kinetic diameter less than the zeolite pore was determined by both diffusion and adsorption properties. Figure 7 shows the relation of permeances with kinetic diameters of CH_4, CO_2, CO and H_2 through the zeolite membrane at room temperature. If we suppose that the as-synthesized zeolite membrane was defect-free, we have a perfect zeolite NaY structure with pore diameter (0.7 nm) larger than the kinetic diameters of CH_4, CO_2, CO and H_2 molecules. In such a case, the effects of molecular sieving play a negligible role in determining the gas separation factor. The permeance could increase or decrease with increasing temperature, depending on the contribution of adsorption to permeances. Bai *et al*. [25] and Baker *et al.* [26] reported the results of gas permeance of silicalite membranes; they observed that the permeances of small molecules went through a minimum with temperature change. In addition, other studies [27] suggested that the permeance of N_2 and H_2 decreased with increasing temperature, in agreement with our experimental results.

The ideal separation factors for CH_4, CO_2, CO and H_2 are shown in figure 8. The results demonstrated that for CO/CO_2, CO/CH_4 and H_2/CH_4 but not for H_2/CO_2, the ideal separation factors exceed the Knudsen diffusion

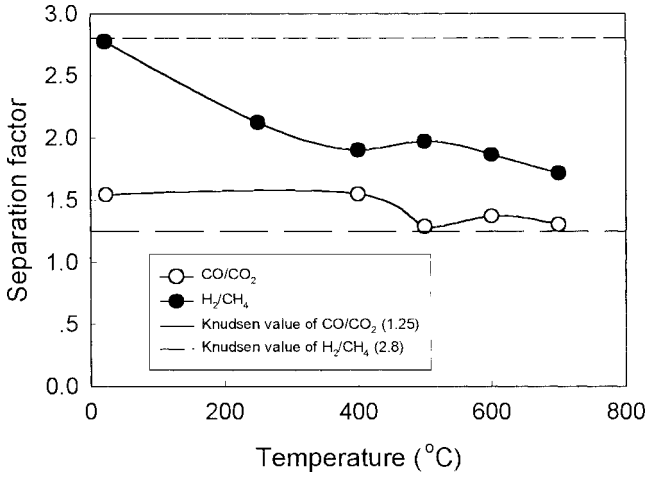

Figure 9. Separation selectivity for 25/25 binary gas mixtures through the zeolite membrane as a function of temperature.

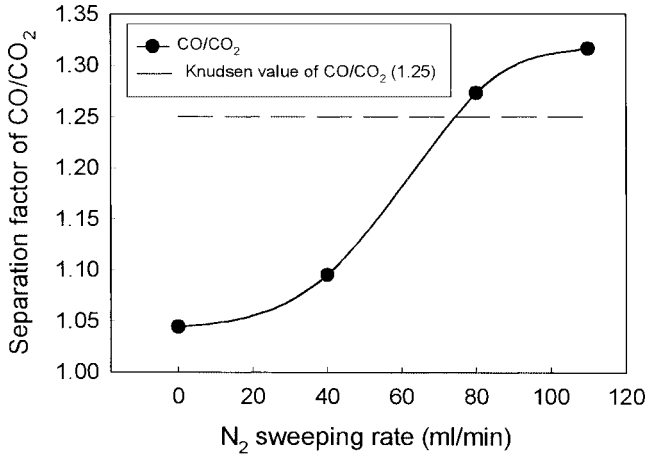

Figure 10. Effect of N_2 sweeping rate on CO/CO_2 separation factor.

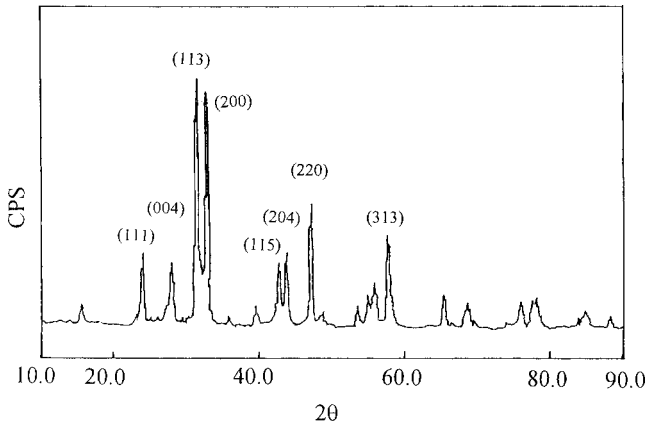

Figure 11. XRD spectrum of La_2NiO_4 membrane powder.

value in the 25–700 °C range. The separation factors, however, decreased with increasing temperature. This behavior could be related to the adsorption capacity of the gas molecules in the zeolite pores, for example, compared to H_2, methane was more strongly adsorbed at elevated temperatures. Dalmon and coworkers [28] studied the permeance and separation performance of hydrogen/isobutane through MFI-zeolite membranes; below 700 K, they reported a reduction in hydrogen flux through the MFI-zeolite membranes with temperature rise. The separation factor of H_2/CH_4 or H_2/CO_2 reported here is significantly higher than that observed previously over ZSM-5 membrane [29].

3.3. Permeaselectivity of binary gas mixtures

The separation for the H_2/CH_4 or CO/CO_2 binary gas mixtures was performed through the zeolite membrane, and the separation factors obtained are shown in figure 9. The results indicate that the separation factor of CO/CO_2 was higher whereas that of H_2/CH_4 was lower than the corresponding Knudsen diffusion values. This is because the strong adsoption of hydrocarbon hinders the diffusion of hydrogen through the zeolite membrane. Therefore, the separation factor of binary gas mixtures was obviously lower in comparison with the ideal separation factor of single gas through the membrane, very much different from the case of hydrogen-selective membranes [17,30]. Since the CO_2 reforming of methane over a fixed-bed reactor [31] was generally performed at 700 °C, the performance of the zeolite membrane at 700 °C was a matter of concern.

Figure 10 shows the effect of sweeping rate of N_2 on the separation factor of CO/CO_2. The results implied that with the enhancement of N_2 sweeping rate, the gas in the permeation side was carried away quickly and the separation factor for the binary gas mixtures increased. That is to say, with a N_2 sweeping rate at or above 80 ml min^{-1}, the separation factor of CO/CO_2 exceeds the value of Knudsen diffusion.

3.4. CO_2 reforming of methane over fixed-bed and zeolite membrane reactors

The XRD pattern of the La_2NiO_4 membrane powder is shown in figure 11. The results indicated a unique tetragonal structure of K_2NiF_4 (spinel) of excellent crystallinity, indicating that it is possible to prepare the La_2NiO_4 spinel structure by mixing La^{3+} and Ni^{2+} in molecular level according to Pechini's approach [32]. La_2NiO_4 is a structure suitable for the stabilization of nickel ions in the catalytic membrane.

The conversions of CH_4 and CO_2 observed over a fixed-bed and a zeolite membrane reactor as a function of reaction temperature are shown in figure 12. At 400 °C, the conversion of CH_4 and CO_2 observed over the zeolite membrane reactor was nearly the same as that observed over the fixed-bed reactor. This is because the activities of the catalyst and catalytic membrane were low at low temperature and a large amount of CH_4 and CO_2 ran off without being reacted. However, above 400 °C, the conversions of CH_4 and CO_2 over the membrane reactor increased remarkably in comparison with those observed over the fixed-bed reactor. At 700 °C, the conversions of CH_4 and CO_2 over the former were 70.96 and 72.7 mol%, respectively, whereas those over the latter were 49.5 and 66.7 mol%. This is be-

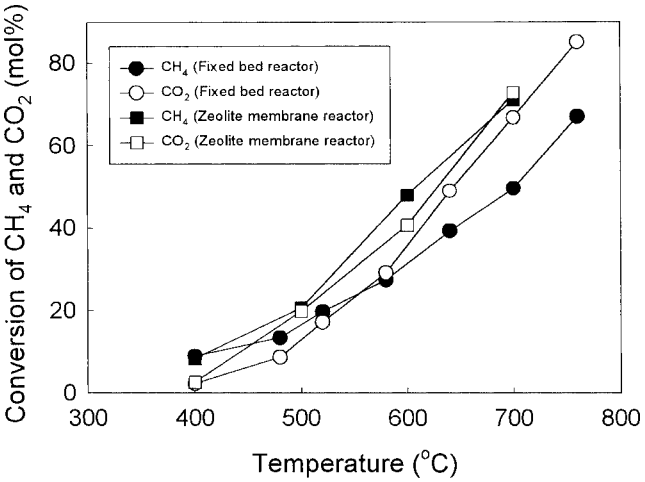

Figure 12. Conversion of CH_4 and CO_2 *vs.* reaction temperature. GHSV = 4.8×10^4 ml g^{-1} h^{-1}, sweeping rate of nitrogen = 80 ml min^{-1}.

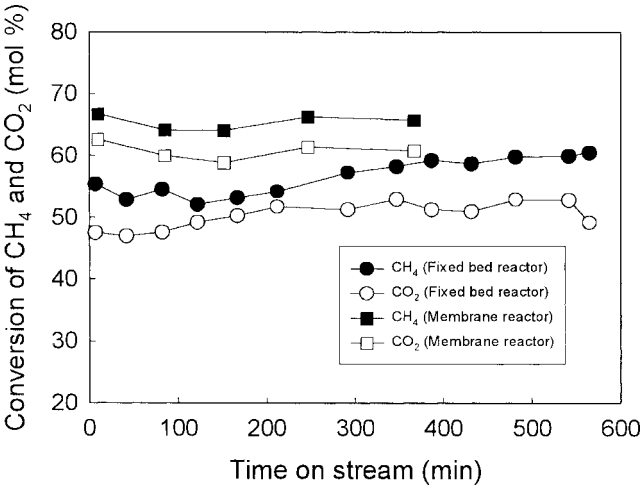

Figure 13. Catalytic activity *vs.* time on stream for both fixed-bed and zeolite membrane reactors. GHSV = 4.8×10^4 ml g^{-1} h^{-1}, sweeping rate of nitrogen = 80 ml min^{-1}, T = 700 °C.

Table 1
Product distribution in CH_4/CO_2 reforming over zeolite membrane reactor.

Temp. (°C)	CH_4 conv. (mol%)	CO_2 conv. (mol%)	Product distribution (mol%)				H_2/CO
			H_2	CO	CH_4	CO_2	
400	8.27	2.53	6.83	4.95	42.91	45.40	1.38
500	20.61	19.74	19.07	16.91	33.01	31.01	1.13
600	47.94	40.61	33.73	31.87	16.17	18.23	1.06
700	70.96	72.72	38.65	44.61	8.10	8.64	0.87

cause the effect of zeolite membrane on hydrogen separation further promoted CH_4 decomposition over the NiO–La_2O_3/γ-Al_2O_3 catalyst.

The product distribution for CH_4/CO_2 reforming observed over the zeolite membrane reactor under the condition of $n(CH_4)/n(CO_2) = 1:1$, GHSV = 4.8×10^4 ml g^{-1} h^{-1}, suggested a H_2/CO ratio of about 1.0 at 500–700 °C (table 1). At 700 °C, syngas was up to 83.3 mol% at high space velocity, and the catalytic activities of the catalyst and the catalytic membrane remained rather stable within 10 h of reaction time (figure 13). For the CO_2 reforming of methane, the conversions of CO_2 and CH_4 observed over the zeolite membrane reactor was remarkably higher than those observed over the fixed-bed reactor. As shown in figure 9, the separation factors of CO/CO_2 and H_2/CH_4 binary gas mixture were not significantly high; besides CO and H_2, CH_4 and CO_2 also diffused towards the outer tube of the zeolite membrane. For the enhancement of CH_4 and CO_2 conversions, the zeolite membrane with catalytic activity exhibited an obvious effect on the reforming reaction, leading to the results observed.

4. Conclusion

The zeolite membrane with catalytic activity was prepared by means of *in situ* hydrothermal synthesis. The results of XRD and SEM-EDX indicated that the zeolite NaY crystallines in well-defined octahedral planes were mainly formed on α-Al_2O_3 support with the presence of zeolite P particles as a contaminant. The average size of the particles was within the range of 5–10 μm.

We observed that the ideal separation factors for H_2/CH_4 and CO/CO_2 exceeded the corresponding Knudsen diffusion values. The results of nitrogen-adsorption isotherm and the pore size distribution of the zeolite membranes verified that the diffusion mechanism of the gases through the membranes was controlled by both Knudsen and micropore diffusion.

The zeolite membrane was utilized in a membrane reactor for the CO_2 reforming of methane. We observed that the conversion of CH_4 over the zeolite membrane reactor was 21.4 mol% higher than that over a conventional fixed-bed reactor. The results demonstrated that the use of a zeolite membrane reactor is obviously advantageous for CO_2 reforming of methane.

Acknowledgement

This work was supported by the Research Grants Council of the Hong Kong Special Administration Region, China (Project No. HKBU 2053/98 P).

References

[1] J.D. Fish and D.C. Hawn, J. Sol. Energy Eng. 109 (1987) 215.
[2] J.H. Edwards, K.T. Do, A.H. Maitra, S. Schuck and W. Stein, Sol. Eng. 1 (1995) 389.
[3] J.R.H. Ross, A.N.J. Van Keulen, M.E.S. Hegarty and K. Seshan, Catal. Today 30 (1996) 193.
[4] M.A. Vannice, Catal. Rev. Sci. Eng. 14 (1976) 153.
[5] H.Y. Wang and C.T. Au, Appl. Catal. A 155 (1997) 239.
[6] A. Erdöhelyi, J. Cserényi and F. Solymosi, J. Catal. 141 (1993) 287.
[7] L. Basini and D. Sanfilippo, J. Catal. 157 (1995) 162.
[8] M.F. Mark and W.F. Maier, J. Catal. 164 (1996) 122.
[9] J.R. Rostrup-Nielsen and J.H. Bak Hansen, J. Catal. 144 (1993) 38.
[10] V.R. Choudhary, B.S. Uphade and A.A. Balhekar, J. Catal. 163 (1996) 312.

[11] P.H. Bolt, F.H.P.M. Habraken and J.W. Geus, J. Catal. 151 (1995) 300.
[12] S.L. Jorgensen, P.E.H. Nielsen and P. Lehrmann, Catal. Today 25 (1995) 303.
[13] J. Galuszka, R.N. Pandey and S. Ahmed, Catal. Today 46 (1998) 83.
[14] Y. Yan, M.E. Davis and G.R. Gavalas, Ind. Eng. Chem. Res. 34 (1995) 1652.
[15] M. Matsukata, N. Nishiyama and K. Ueyama, J. Chem. Soc. Chem. Commun. (1994) 339.
[16] H. Kita, K. Horii, Y. Ohtoshi, K. Tanaka and K. Okamoto, J. Membr. Sci. Lett. 14 (1995) 206.
[17] B.S. Liu, G.H. Wu, G.X. Niu and J.F. Deng, Appl. Catal. A 185 (1999) 1.
[18] P. Thompson, D.E. Cox and J.B. Hastings, J. Appl. Crystallogr. 20 (1987) 79.
[19] A.R. Armstrong, P.A. Anderson, L.J. Woodall and P.P. Edwards, J. Am. Chem. Soc. 117 (1995) 9087.
[20] L.V. Interrante and L.A. Caspar, *Materials Chemistry*, Adv. Chem. ser. 245 (Am. Chem. Soc., Washington, DC, 1995) ch. 22, p. 330.
[21] K.S.W. Sing, D.H. Everett, R.A.W. Haul and L. Moscou, Pure Appl. Chem. 57 (1985) 603.
[22] S.J. Gregg and K.S.W. Sing, *Adsorption, Surface Area and Porosity*, 2nd Ed. (Academic Press, London, 1982).
[23] G.D. Halsey, J. Chem. Phys. 16 (1948) 931.
[24] Y.S. Yin and A.J. Burggraaf, J. Membr. Sci. 79 (1993) 65.
[25] C. Bai, M.D. Jia, J.L. Falconer and R.D. Noble, J. Membr. Sci. 105 (1995) 79.
[26] W.J.W. Bakker, F. Kapteijn, J. Poppe and J.-A. Moulijn, J. Membr. Sci. 117 (1996) 57.
[27] A. Giroir-Fendler, J. Peureux, H. Mozzanega and J.-A. Dalmon, Stud. Surf. Sci. Catal. 101 (1996) 127.
[28] P. Ciavarella, H. Moueddeb, S. Miachon, K. Fiaty and J.-A. Dalmon, Catal. Today 56 (2000) 253.
[29] J. Coronas, J.L. Falconer and R.D. Noble, AIChE J. 43 (1997) 1797.
[30] B.S. Liu, H.X. Li, Y. Cao, J.F. Deng, C. Sheng and S.Y. Zhou, J. Membr. Sci. 35 (1997) 33.
[31] J.Z. Luo, Z.L. Yu, C.F. Ng and C.T. Au, J. Catal. 194 (2000) 198.
[32] M.P. Pechini, US Patent 3 330 697 (1967).